SEM Dopant Contrast due to Patch Fields in Semiconductors

pr59

15 Mar 2002

Contents

Chapter 1

Abstract

When semiconductors are observed in Scanning Electron Microscopes (SEMs), variation in doping concentration causes a variation in the detected secondary electron signal. If the mechanisms for this are properly understood, it may be possible to use the SEM for very quick compositional analysis of these specimens.

One proposed mechanism for this doping contrast is that the local electric field at the interface between two differently doped regions (caused by the built-in voltage) deflects electrons and alters their trajectories, so that the number of electrons reaching the detected is affected. Note that this needs to be distinguished from 'ionisation energy contrast', which also depends on the the built-in voltage and local fields. We did some experimental work to try discover whether this mechanism was responsible for some of the contrast seen, which was cut short by equipment failure, but, in view of the later theoretical work, showed that this mechanism is not the major mechanism for contrast.

We then produced a model for the simple case of a p-n junction with a realistic microscope geometry, and ran simulations to test the mechanism theoretically. We determined semi-quantitatively its dependence on various parameters, including the work function of the material, the built-in voltage of the junction and the extractor voltage.

We found that for a typical silicon p-n junction under typical operating conditions, there was a contrast of about -2.5% between the two sides of the junction (using the normal sign convention), which was in the sense that would be predicted for this mechanism, but is opposite to that normally seen. However, it was also found that this contrast was very sensitive to operating conditions, and could in fact be reversed as far as +9%. This showed that this mechanism, although not entirely responsible for the contrast seen, can play a significant part, and therefore cannot be neglected. The sensitivity to operating conditions and geometry of the microscope means that unfortunately this mechanism will be a hindrance to any quantitative analysis being attempted. However, we also found that for a typical case, an extractor voltage of about 140V (which is well within the limits of the kind of microscope used) virtually eliminates this type of contrast.

Chapter 2

Nomenclature

The following symbols and abbreviations are used throughout this report. They are always explained in the first instance of use, and this is included for reference. Note that in some cases there is duplication of symbols, simply to keep with convention used. In context, there is little chance of confusion. Note also that in the computer program, longer names are often used.

BSE	Back Scattered Electrons—electrons from the primary beam that are 'reflected' from nuclei in the sample
e	magnitude of electronic charge $= 1.6 \times 10^{-19}$
E	Energy of the emitted SE or other specified energy
E_{SE}	Energy of the emitted SE
$\mathbf{E}$	Electric field vector
E_x, E_y, E_z	Cartesian components of the electric field
$E_{extract}$	The extractor field caused by $V_{extract}$
m_e	mass of an electron $= 9.1 \times 10^{-31}$
PE	Primary Electrons—the incident beam of electrons, generated by the SEM
q_e	electronic charge $= -1.6 \times 10^{-19}$
SE	Secondary Electrons—those ejected from the sample by the primary beam
SEM	Scanning Electron Microscope
TLD	through-lens detector
V	electrostatic potential
x, y	Cartesian coordinates of an emitted electron, where the y-axis is coincident with the centre of the accelerating column of the SEM, the origin is on the surface of the sample, and the x-axis is perpendicular to the p-n junction interface
α	the angle the initial trajectory of an SE makes with the surface normal
ϕ	work function of the material
V_{BI}	the built-in voltage across a p-n junction

Chapter 3

Introduction

3.1 Scanning Electron Microscopes

Scanning Electron Microscopes (SEMs) are used in a variety of ways to collect information about a sample. The most common and well-known mode is where the intensity of secondary electrons (SEs—those ejected from the sample by the incoming beam) is collected and measured for each point over a rectangular area to build up an image. Other signals that can be collected include back-scattered electrons (BSE) and Auger electrons, and as well as measuring intensity, the energy spectrum can also be measured using techniques such as EDX. This project is concerned with only the intensity of the SE signal, and it is assumed that the reader is familiar with the basic concepts and design of an SEM.

The SE signal is normally used to get topographic information. Topographic features can hinder electrons from reaching the detector and thus create 'shadows' on the image formed—this is known as topographic contrast. The intensity of the SE signal is also affected by various material properties:

- Work function—a higher work function means that more energy is required to remove electrons from the surface, and thus the yield decreases. The energy spectrum of the emmitted SEs is also strongly affected (see section 5.2.1).
- Atomic weight A, atomic number Z and density ρ—these effect the penetration of the primary beam into the sample, and thus the region over which SEs are emitted. The range equation gives the following for the width and depth of the interaction volume:

  $$R = \frac{0.0276AE^{1.67}}{Z^{0.89}\rho}(\text{in } \mu \text{ m})$$

  These properties can therefore affect the intensity of signal produced on a specimen.

Since the 1970's, it has been found that variations in dopant concentration in semiconductors can also produce contrast in the SE signal (Lifshin *et al*, 1972[3], Aven *et al*, 1972[4], etc.). This contrast cannot be explained by any of the mechanisms listed above. The variation in composition is far too small to be responsible for the contrast to be a result of changes in material properties.

If dopant contrast can be characterised and explained, it could form the basis of a very quick and convenient method of quantitative dopant profiling, which is the driving force behind this research. Various mechanisms are thought to be responsible for dopant contrast. These are discussed briefly below, in

particular the mechanisms relating to patch fields, since these are the basis of the mechanism under investigation in this report. A more detailed discussion of most of these can be found in *Dopant Profiling with the Scanning Electron Microscope* by Elliot[1] and in *Scanning Electron Microscopy—Physics of Image Formation and Microanalysis* by Reimer[6].

3.2 Dopant Contrast Mechanisms

3.2.1 Voltage contrast

This includes a number of different situations. Variations in the potential of the surface of a specimen can arise either accidentally (due to surface charging for example), or deliberately (e.g. by biasing of integrated circuits). The surface potential of regions can then repel or attract the electrons emitted, and so change the number that escape and their energies, and also their trajectories[6]. Applying a bias voltage to the detector will also produce the same effect, but globally across the specimen, and this is included under voltage contrast. An applied extractor voltage is almost always used to improved detecter efficiency.

3.2.2 Surface states and band-bending

When a semiconductor is cleaved, the presence of the surface means that extra electronic states are produced, on top of those in the bulk material. For an n-type semiconductor, energy minimisation means that charge flow tends to occur towards the surface, until an equilbrium is set up such that the electric field caused by the excess negative charge balances the movement of electrons. Thus there is a depletion of electrons in the bulk and there is a resultant bending of the electron energy bands. An equivalent but reversed effect is seen in p-type semiconductors, where the surface becomes positively charged and the bands bend in the opposite direction. The net effect is that the surface of an n-type semiconductor becomes negatively charged and the surface of a p-type semiconductor become positively charged. This surface charge affects the energy needed for SEs to escape from the surface of the crystal. This was first proposed by Perovic, 1995[5].

3.2.3 Patch fields—ionisation energy contrast

Patch fields relate to contrast between materials of different work function, but due to the materials being put in contact (as opposed to the effect that would be seen if they remained separate, see above). If the materials are (semi)conductors, then the Fermi levels of the two materials will equalise on contact, by the movement of electrons from one to the other. This means that in the case of a region of lower work function being surrounded by a region of higher work function, the region of lower function will become positively charged, and the surrounding region negatively charged—see figure 3.1. There will therefore be a potential barrier for electrons to escape from the region of lower work function. As a result of the electric charge distribution on the surface of the crystal, an electric field will exist outside the crystal, called the patch field.

A detailed analysis of the case of a p-n junction has been done by Sealy *et al* [7]. In a p-n junction, a 'built-in' voltage V_{BI} develops at the junction when the p- and n-type semi-conducting materials are placed in contact. The Fermi levels on the two sides equalise by a flow of electrons from the n-type to the p-type. As electrons diffuse into the p-type material, they combine with the excess holes in the p-type and annihilate them. Similarly holes diffuse

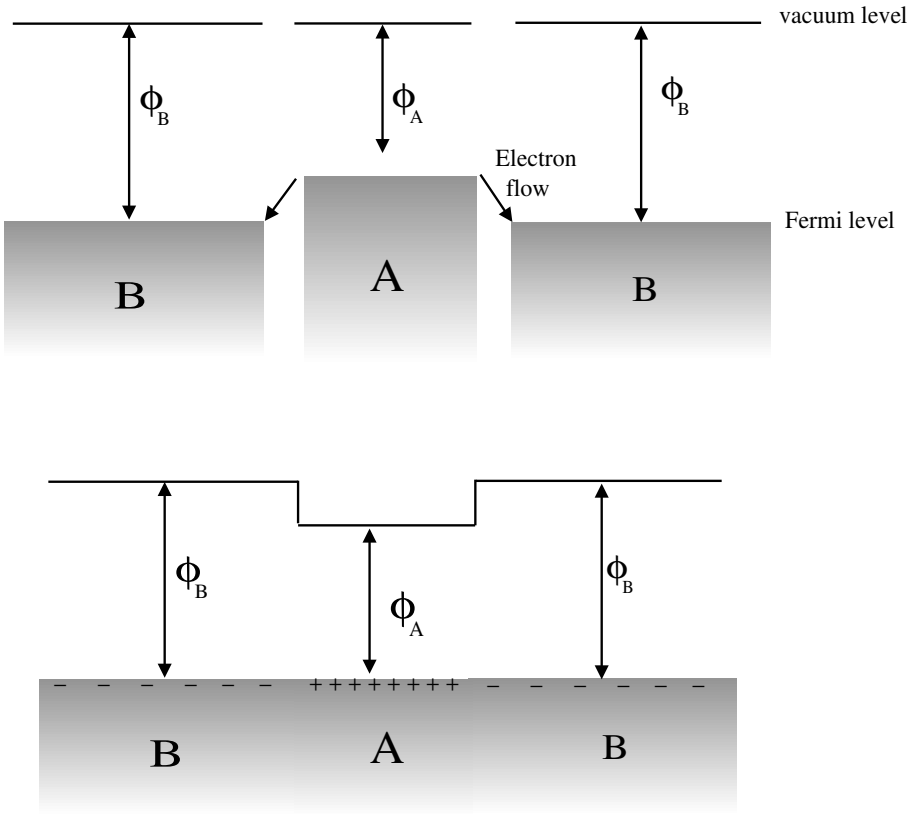

Figure 3.1: Schematic of the energy bands of a material A surrounded by material B with a higher work function, before and after contact. The Fermi levels equalise, so that region A becomes positively charged. Patch fields must arise because of the surface charges (Taken from Elliot[1])

into the n-type region and annihilate the free electrons. Since these holes and free electrons were associated with acceptor and donor atoms respectively, their removal produces charges that are at fixed positions in the lattice. Thus a region of 'space-charge' either side of the junction is created (see figure 3.2). This generates an electric field which opposes the further diffusion of carriers until an equilibrium is reached. This 'built-in' electric field has an associated 'built-in' voltage V_{BI}, such that the electrostatic potential of the n-type side is raised by V_{BI} (and the electron energy of the n-type side is lowered by an energy $E_{BI} = eV_{BI}$).

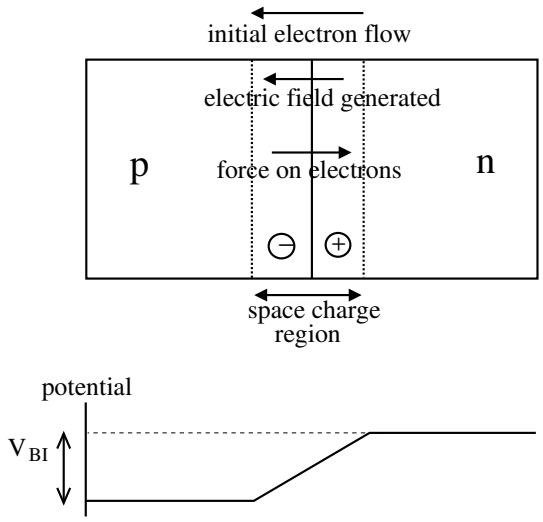

Figure 3.2: Schematic showing the space-charge (carrier depletion) region in a p-n junction and the electric field that develops as soon as contact is made. Taken from *Introduction to applied solid state physcis*, Dalven[8]

The built-in voltage in a p-n junction means that patch-fields must exist outside the surface of the junction, and that there must be a potential barrier for electrons leaving the semiconductor. Sealy *et al* showed that for a p-n junction with equal areas of p- and n-type material, given certain other assumptions, the potential barrier for n-type is $1/2E_{BI}$ larger than that for p-type (see figure 3.3). The result of this is a type 'ionisation energy contrast'—the p-type side will emit SEs more easily and therefore appear brighter, producing contrast between the two sides.

Sealy also showed that the presence of surface states and band bending, as described above, will affect this, and actually decrease the contrast that is seen. There is significant, though not conclusive, experimental evidence for this mechanism both qualitatively and quantitatively—p-type doped semiconductors in general appear brighter in the SEM than the undoped material, and n-type doping makes the material appear darker, and in some cases the contrast follows the logarithmic dependence on doping levels that is predicted.

3.2.4 Patch fields—trajectory contrast

The patch fields described above may have another effect on the contrast. It was realised in 1969 by Plows that this external field could cause deflection of electron trajectories in SEMs[2], but there was not enough computational power available to calculate how large this effect would be. In fact there are

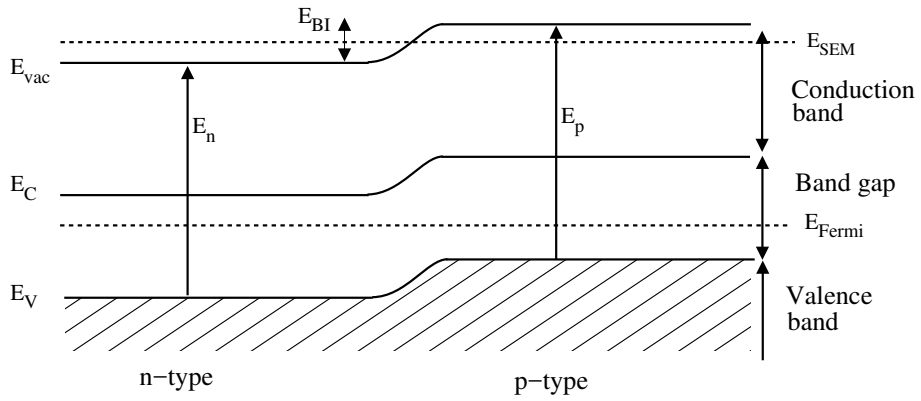

Figure 3.3: Energy bands in a p-n junction. E_{SEM} is the far-field vacuum level. For SE emission, an electron must overcome the local potential barrier: for n-type, this is from E_V to E_{SEM} which equals $E_n + 1/2E_{BI}$; for p-type, this is from E_V to the local E_{vac} which equals E_p. E_{BI} is the energy associated with taking an electron through the built-in voltage, $E_{BI} = eV_{BI}$. We can assume that $E_p = E_n$. (Taken from Sealy[7])

two contributions to this mechanism: the incoming (PE) and outgoing (SE) beams will both be deflected. However, the incoming beam will generally be of sufficiently high speed and energy that this deflection can be neglected, and here only the latter will be investigated.

This deflection of electrons due to local fields on the surface of the object is known to operate in general terms. For example, negatively charged dust particles on the surface of a sample cause a dark 'shadow' as the electron emission is hindered in surrounding regions by the distortion of the electric field[6].

Plows did a large amount of theoretical work on the form of the electric field above the surface of a p-n junction. A simplification of his result forms the basis of the model used below.

It appears that relatively little has been done on the quantitative magnitude of contrast that would be expected due to this mechanism in the context of doping contrast, and this was the main focus of my project. An attempt was made to determine the magnitude of this mechanism theoretically (for the specific microscope geometry and conditions used), and to do experimental work to back this up. Given that there is little proof for the other mechanisms, and they have not always been consistent with experimental results, it could be that this mechanism is in fact a major contribution.

Chapter 4

Experimental work

It was suggested that the 'trajectory contrast' would vary considerably with the extractor bias (voltage) of the detector. The reason for this is that a large extractor voltage will swamp any local field effects, and thus reduce the contrast from this mechanism, while a low (or zero) extractor voltage will produce trajectories that are entirely dependent on the local fields. The first, and only, experiment to be done attempted to find how the doping contrast varied with extractor bias. Equipment failure then prevented further experimental work.

The sample used for the experimental work was not ideal, as it was more complex than the familiar p-n junction. The SIMS profile is given in figure 4.1. It consisted of several layers of p-type doped layers on a silicon substrate. If time and equipment had allowed, a more suitable sample would have been prepared.

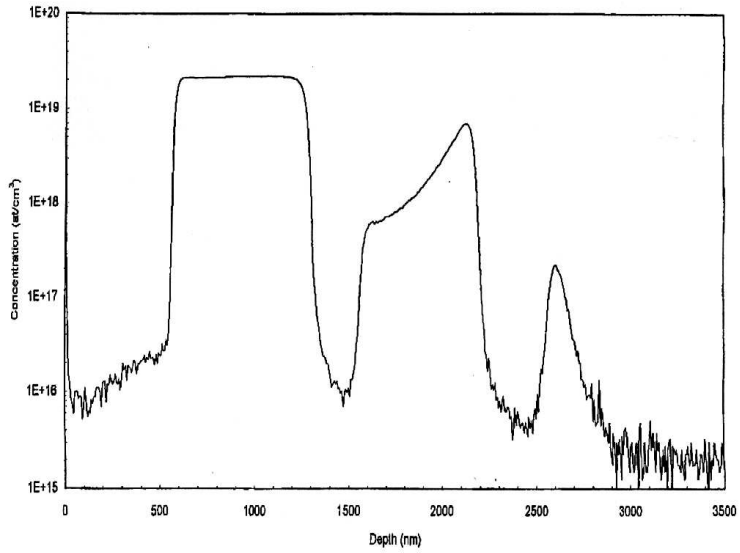

(c) SIMS profile for the p-layers of SLE008

Figure 4.1: SIMS profile of the specimen used—it is B-doped Si, sample SLE008 in S. L. Elliott's PhD.

4.1 Method

4.1.1 Sample preparation

The specimen was cleaved in air to produce a long surface with no visible defects (such as steps on the surface). When satisfied that a good surface had been obtained, venting of the microscope chamber was begun immediately. The longer the specimen is kept in air, the more it degrades in quality, so this time must be minimised. However, the microscope chamber should also be kept under vacuum as long as possible to prevent adsorption of water and other gases onto its surfaces, which will harm the performance of the microscope. Therefore the chamber cannot be vented earlier, and this is the best compromise of these two requirements.

The sample was then loaded into the microscope with the surface approximately horizontal. The tilt would be further adjusted once inside to ensure it was as close to horizontal as possible.

The specimen was always handled while wearing latex gloves, and the surface that was to be examined was never touched even with the gloves, as this will ruin the surface.

4.1.2 Examination

When collecting images, a number of precautions were taken to ensure that good data was obtained.

- The TLD (through-lens detector) was always used for taking any information that needed to be quantitative, and was generally used as soon as the operating conditions (such as magnification and working distance) allowed. The TLD was used as it is known to be much better suited for viewing the dopant contrast. For our purposes it is also far easier to model theoretically than the more usual detector in SEMs.

- The doping layers in the sample were all parallel to the long edge of the sample. Therefore the sample was arranged in the SEM so that the long edge was as close as possible to parallel with one of the sides of the image (viewing screen). This allowed numerical analysis to be done much more easily.

- The accelerating voltage chosen was 0.78 kV. This was chosen as it had been empirically found before to be the value that minimized charging of the sample. (In fact, for our sample some charging was observed).

- Increasing the magnification and focussing was done as soon as possible, without leaving the microscope scanning over large regions of the specimen. This is done because the very act of scanning the electron beam over the surface degrades the quality of the images that can be obtained by causing carbon (present as trace amounts of hydrocarbon gas in the chamber atmosphere) to be be deposited on the surface. For the same reason, when taking images, a new region of surface was always taken, and the image was taken as soon after having switched to the new region as possible. Figure 4.2 shows an image of region that had been scanned for a few seconds, and then the magnification decreased—the carbon deposits can clearly be seen as the darker central region.

- The images taken for quantitative analysis were taken using a slow scan to reduce noise. Before switching to the slow scan, a fresh region of the

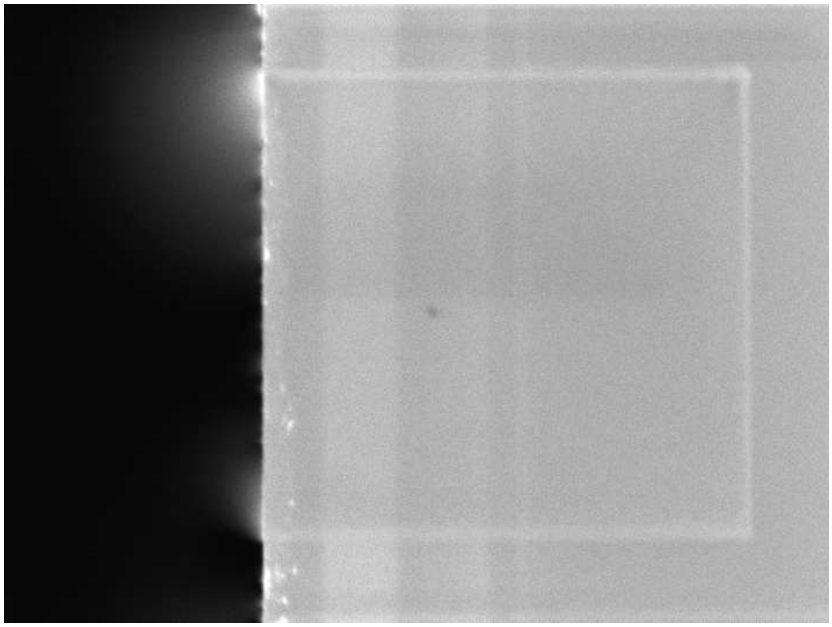

Figure 4.2: SEM image showing the effect of carbon deposition due to scanning of the beam

sample would be briefly scanned in TV mode to look for the presence of dirt or defects that would ruin the data.

- All the usual focussing and correction of stigmatism was done.

The aim was to measure the contrast as a function of extractor voltage. To measure the contrast two images are needed: first, an image of the sample must be taken in which the contrast and brightness for the significant portion of the image have been adjusted so that the signal is within the upper and lower signal limits; second, a 'beam blanked' image is taken, which gives the background intensity level, and must be 'subtracted' from the first image. From the resultant image, the contrast between the doped layer and the substrate can be calculated. The value obtained this way will be independent of the contrast and brightness settings of the microscope.

To help these requirements, the contrast and brightness signals were adjusted so that the signal was in the correct range for the entire range of extractor bias values. This makes taking the measurements more convenient as very little needs adjusting, at the expense of slightly higher accuracy that could be obtained if they were readjusted for every case.

With all these things in mind, images for different extractor biases (from 0V to 240V) were taken. The image for 60V is shown in figure 4.3 as an example. Figure 4.4 shows another image of the same sample at a lower magnification which shows the scale of the doping layers (this image was not used for quantification).

4.1.3 Analysis

For each image, the many rows of data were combined to get an average of all the rows, and thus increase the amount of data that was used and condense it into a single plot of intensity against position (see figure 4.5 for an example).

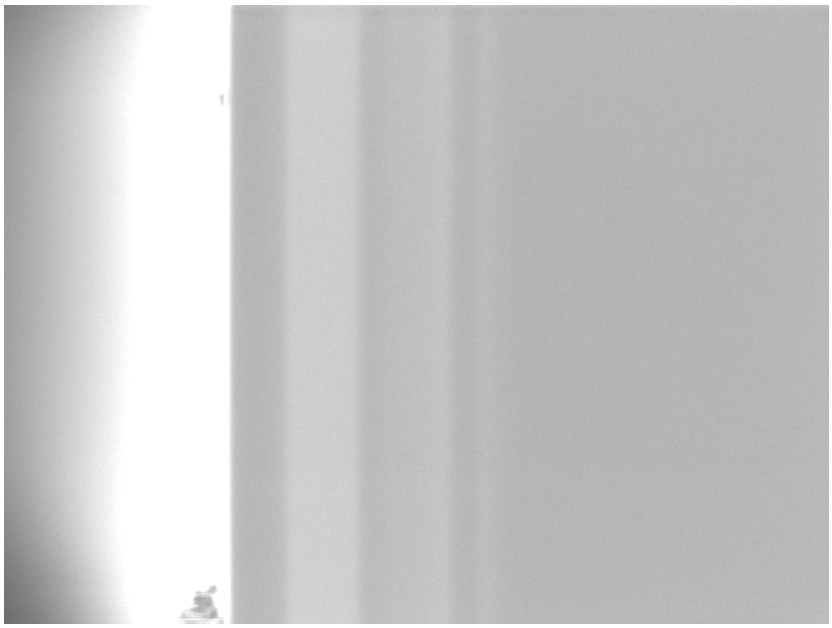

Figure 4.3: Example SEM image used for quantitative analysis

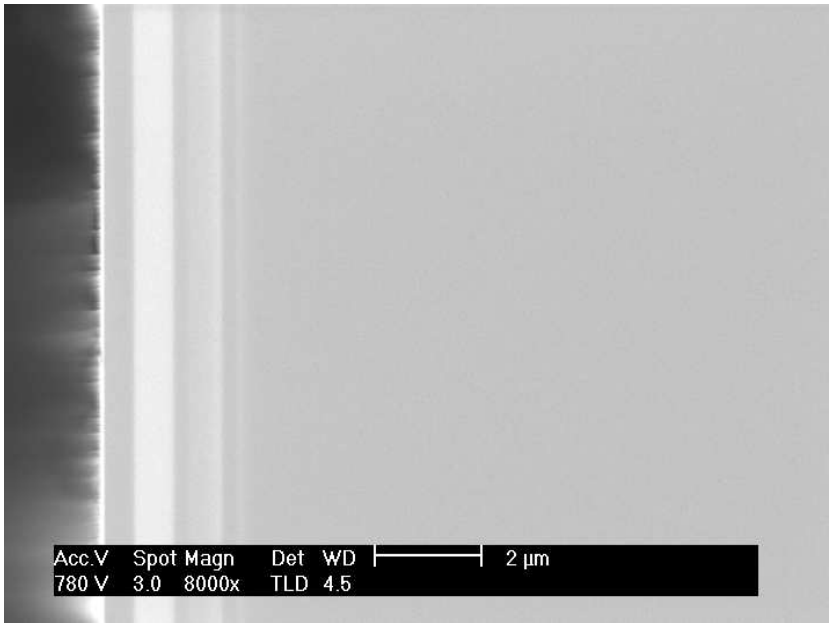

Figure 4.4: Example SEM image

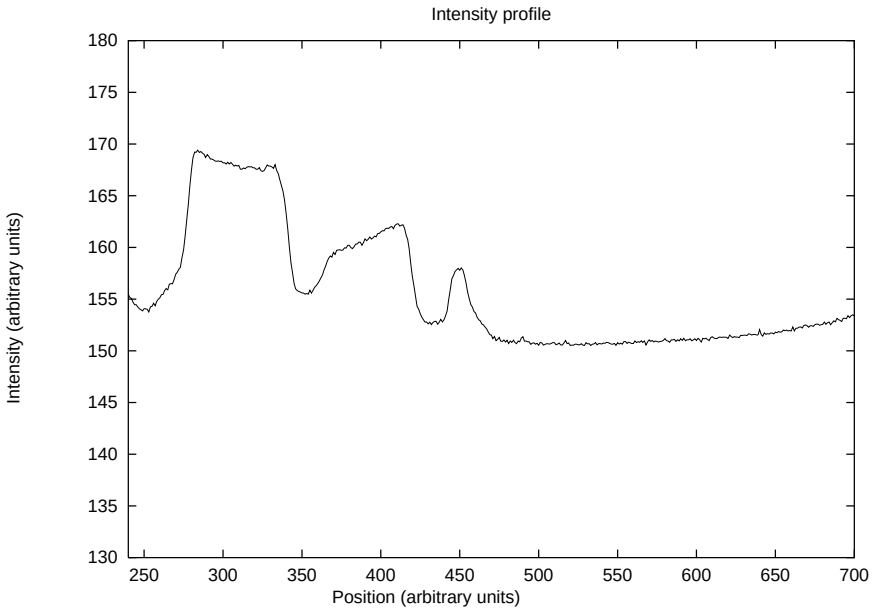

Figure 4.5: Intensity against position for zero extractor bias. The position is in arbitrary units (in fact pixels)

Using the data from these plots, the contrast between the first doped region and the substrate was calculated in each case. An estimate of the error was found by looking at the variation in the intensity across these two regions (which both had constant concentrations of dopants according to the sample specifications).

4.2 Results

The values of contrast and their errors were calculated for each value of extractor bias that images were taken at. The contrast is defined in this case as:

$$C(pi) = \frac{S(p) - S(i)}{S(i)}$$

where 'p' stands for the p-type, i is the intrinsic (undoped material) and S is the signal intensity. The results are given in figure 4.6.

A plot was also made of $S(p)$ and $S(i)$ against the extractor bias, which is included as figure 4.7.

4.3 Discussion

If the trajectory contrast is the main mechanism, it was thought that the contrast should decrease with increasing extractor bias, as explained above. The results clearly do not show a situation that simple, which is due to a number of factors:

- The trajectory contrast is not the only mechanism operating
- In fact, as the theoretical analysis later showed, the contrast we expect from this mechanism is in the opposite sense to that observed.

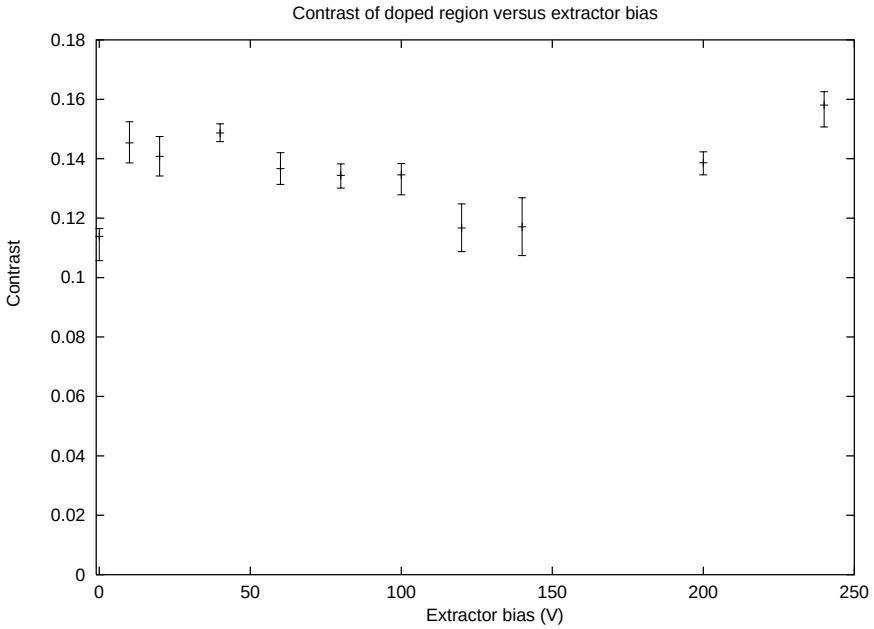

Figure 4.6: The contrast between the doped region and the substrate plotted against the extractor bias.

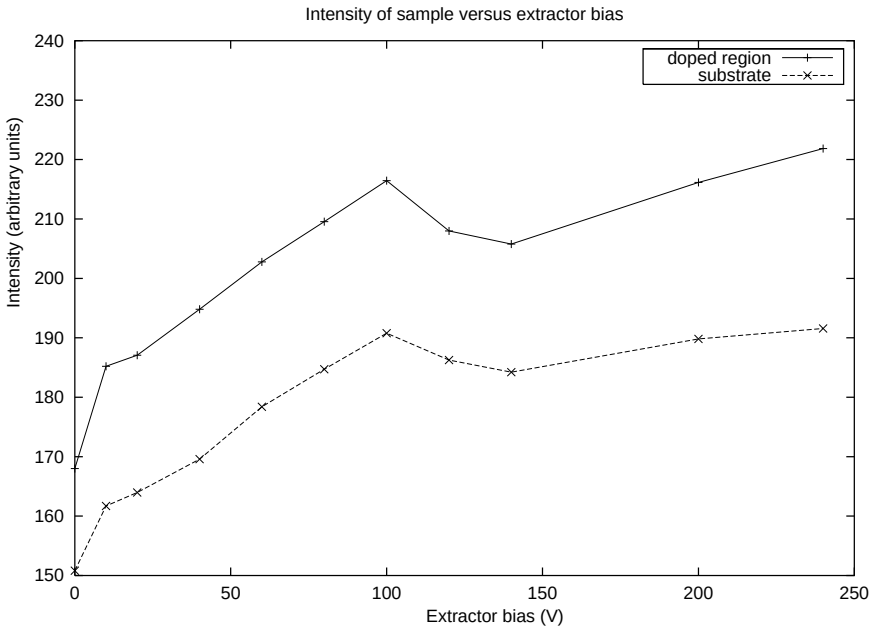

Figure 4.7: The intensity of the doped region and of the substrate plotted against the extractor bias.

- From the theoretical work, the trajectory contrast does not have a dependence on extractor bias that is as simple as expected.

Another observation is that the absolute intensity does not vary as expected either. We expect the intensities $S(p)$ and $S(i)$ to increase with increasing extractor bias, as more electrons will be drawn towards the detector. However, while this is generally true, the results in figure 4.7 show that this, too, is more complicated. An explanation for this has not yet been found, but one suspiscion is that some kind of energy filtering may be at work, seeing that the energy of the electrons reaching the detector will vary with extractor bias and the detector will not be capable of collecting electrons of every energy.

Chapter 5

Theoretical work

The challenge was to model the trajectories of electrons from the surface of the semiconductor to the electron detector, and so to be able to calculate what the contrast would be *for this mechanism only.* Therefore all other contributions to the contrast were deliberately neglected, even though some of them could have been included.

One of the problems is that there are many variables that can be changed and that will vary from machine to machine. It was therefore decided to limit the work to one specific geometry, and also to limit other values to close to realistic values where these were known. The aim was not just to understand how the contrast might vary with the work function of the material, for example, but how large the contrast would be for a specific material and situation.

The dopant profile was also limited to one very specific, but common, case. The one chosen was that of a p-n junction, since this allowed us to make use of the work of Sealy and Plows, and anything more complicated should only be attempted after this familiar case was analysed and understood.

5.1 Model

The set up of the microscope was greatly simplified to allow it to be modelled. A diagram of the TLD detector is shown in figure 5.1. The detector has a (relatively) complex set of electrodes to deflect electrons into the scintillator. In the model we ignore all of this, and assume that all the electrons that reach the detector height within the detector width will be detected—see 5.2. The x and y axis are also defined in that diagram. It is assumed that the p-n junction remains in this central position and that the electron beam is scanned across it. The width over which the beam will be scanned (at most 100 μm either side of the p-n junction) is small compared to the detector width (5mm), so the exact position of the p-n junction will not make much difference.

The extractor field was modeled as a uniform electric field defined by the extractor voltage divided by the working distance.

The model needs to 'generate' many electrons which are representative of the correct energy distribution and angular distribution, and then trace their paths from their excitation point as they are accelerated by the electric field, until it is determined whether they have reached the detector or not. The fraction of electrons detected will be recorded. To determine the contrast, the fraction of electrons collected must be determined for a range of excitation points either side of the p-n junction. This will result in a plot of intensity against position, from which a value of contrast will hopefully be calculated. Then, different parameters, such as the extractor voltage, can be varied and the effect on the

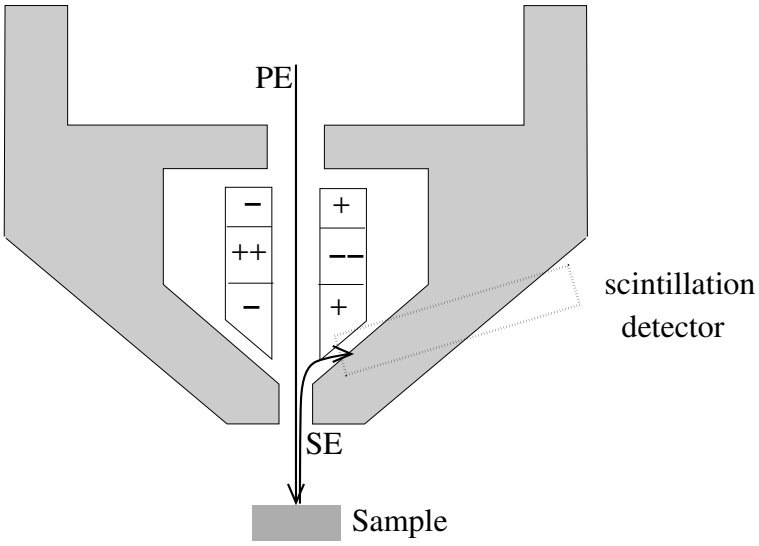

Figure 5.1: Diagram of the TLD detector showing the paths of PE and SE beams.

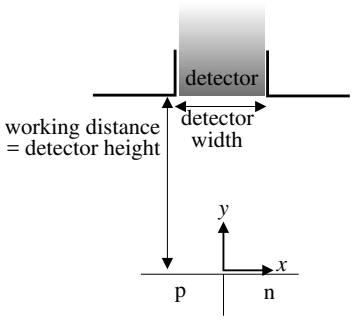

Figure 5.2: Diagram showing the 'detector' defined in the model.

contrast can be found.

5.2 Implementation

A program called `MuPAD` was used to implement this model. This was used as it has a powerful symbolic maths engine, as well as being able to do numerical calculations and plotting. Much of the symbolic integration below was done using the program.

5.2.1 Electron distribution

For secondary electrons (neglecting the high energy backscattered electrons), the energy distribution of the electrons emitted is given below:

$$N(E) \propto \frac{E}{(E+\phi)^4}$$

It is also known that the angular distribution of SEs for this situation, where the incident beam is perpendicular to the surface, is:

$$N(\alpha) \propto cos(\alpha)$$

where α is the angle from the surface normal.

The combined distribution is therefore:

$$N(E,\alpha) \propto \frac{E}{(E+\phi)^4} cos(\alpha)$$

If we want to find the probability that a given electron has a certain energy and angle, we need to normalise:

$$\begin{aligned} p(E,\alpha) &= \frac{\frac{E}{(E+\phi)^4}\cos(\alpha)}{\int_{E=0}^{\infty}\int_{\alpha=-\pi}^{\pi}\frac{E}{(E+\phi)^4}\cos(\alpha)\,d\alpha\,dE} \\ &= \frac{\frac{E}{(E+\phi)^4}}{\int_0^{\infty}\frac{E}{(E+\phi)^4}\,dE}\cdot\frac{\cos(\alpha)}{\int_{-\pi}^{\pi}\cos(\alpha)\,d\alpha} \end{aligned} \tag{5.1}$$

`MuPAD` is able to do this integration. A plot of the form of the resultant distribution is given in figure 5.3.

We then need to generate a number of 'bins' representing ranges of electron energies and angles—the distribution must be split into a number of sections in both the angle and energy direction. The bins must then be filled with an appropriate number of electrons. To do this, we first scale this normalised distribution up by the number of electrons we want to model. We then work out the 'volume' contained in each bin, and round it to the nearest integer to find the number of electrons it should contain. This works well provided that the number of electrons is significantly larger than the number of bins. The actual number of electrons will be different from the scale factor used, due to rounding errors. In the simulations done, a scale factor of 400 was used, with 200 bins, resulting in a total of 342 electrons.

Also, the energy range used was adjusted automatically so that the highest energy bin would contain just one electron, and the one after that would have

contained zero electons. A numerical solver in MuPAD was used to do this. The resulting discretised distribution can be seen in figure 5.4. For each electron, the actual value of energy and angle was picked at random from within the bin it belonged to. Since MuPAD used a pseudo-random number generator which is always seeded with the same value, the actual values used for each electron were identical every time it was run.

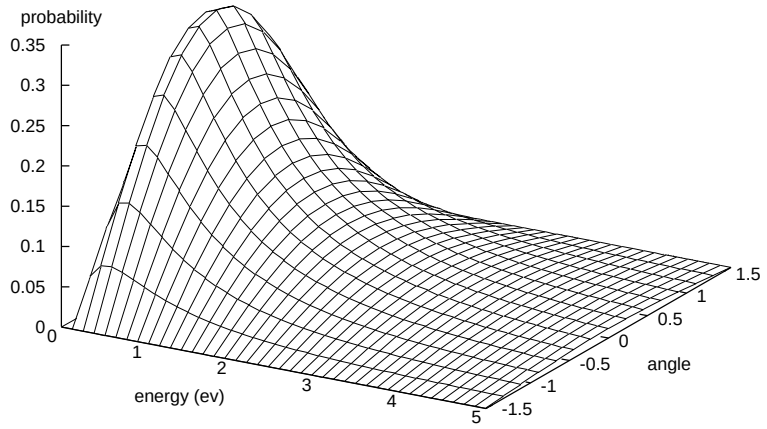

Figure 5.3: Electron probability distribution for a work function of 1eV

5.2.2 Electric field

The form of the potential for the space outside a p-n junction has already been calculated theoretically[2]:

$$V(x,y) = \frac{V_{BI}}{\pi} \arctan\left(\frac{x}{y}\right),\ y > 0$$

The x and y axes are defined as before, with the p-type side being on the negative x side and the n-type along positive x, and the y axis vertical. Note that this model assumes not only an abrupt junction, but an abrupt change in potential at the junction, (it tends to a step function as $y \to 0$) when in reality there is a space-charge region over which the potential decreases.

To this potential, the extractor bias $V_{extract}$, and thus the extractor field $E_{extract}$, needs to be added, giving:

$$V(x,y) = \frac{V_{BI}}{\pi} \arctan\left(\frac{x}{y}\right) - E_{extract} y$$

MuPAD can then calculate the cartesian components of $\mathbf{E}$ by differentiation. We have neglected motion in the z direction since E_z is zero, and assumed that all motion is in the x-y plane, but in fact the z-direction should be included. The electron distribution would need to be modified to include a third dimension—an azimuthal angle for example.

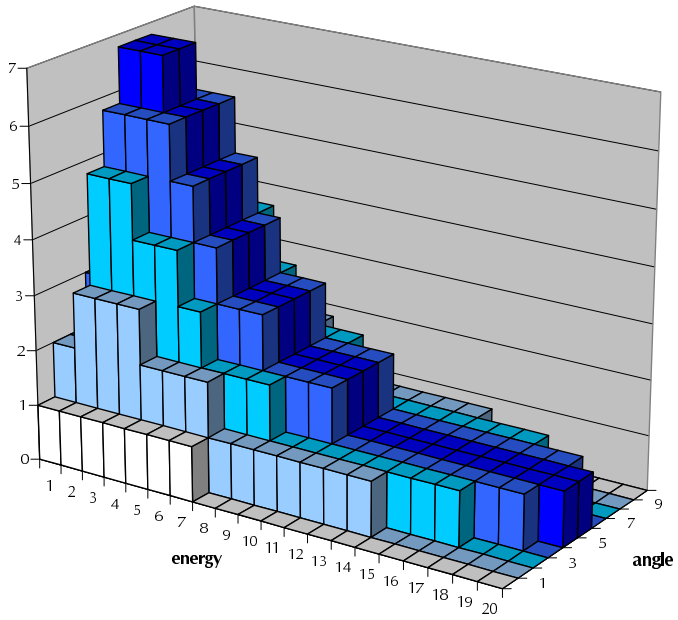

Figure 5.4: Discretised electron distribution containing 342 electrons, with 20 energy bins and 10 angle bins. If the work function is changed, this distribution does not change, only the energies assigned to each bin.

A plot of the form of E_x and E_y as a function of x and y can be seen on figures 5.5 and 5.6. These are useful in predicting the contrast seen (remembering that the force on an electron will be in the opposite direction to the field).

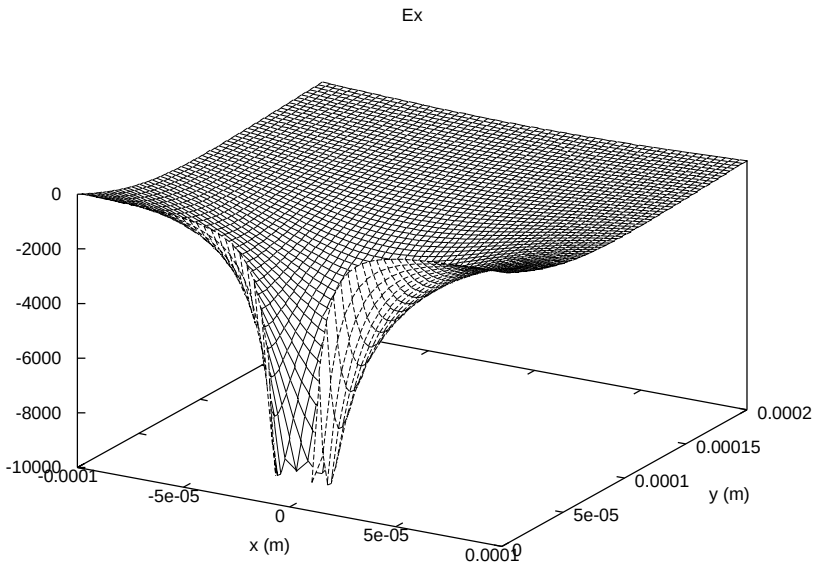

Figure 5.5: Spatial variation of electric field component E_x (values in SI units)

5.2.3 Electron trajectory

This is governed very simply by the equation of motion in two dimensions (since we have neglected the third):

$$m_e \frac{d^2\,\mathbf{r}}{dt^2} = q_e \mathbf{E}(\mathbf{r})$$

where $\mathbf{r} = \begin{pmatrix} x \\ y \end{pmatrix}$

`MuPAD` cannot solve this analytically, but it can solve general first order differential equations of the form $\mathbf{Y}' = f(\mathbf{Y}, t)$ numerically. This second order o.d.e. in 2 dependent variables can be simply converted into a first order in 4 variables:

$$\frac{d}{dt}\begin{pmatrix} x \\ x' \\ y \\ y' \end{pmatrix} = \begin{pmatrix} x' \\ \frac{q_e}{m_e} E_x(x,y) \\ y' \\ \frac{q_e}{m_e} E_y(x,y) \end{pmatrix}$$

which is of the correct form.

This can then be solved numerically, using the initial value of $\mathbf{Y}$ as the initial conditions of integration, to give the x and y coordinate for any value of t. The values of x' and y' are also calculated as a by-product, but are unused.

5.2.4 Electron detection

Assuming that the electron heads upwards, we simply need to find its horizontal position when it is at the detector height to check that it goes through the gap.

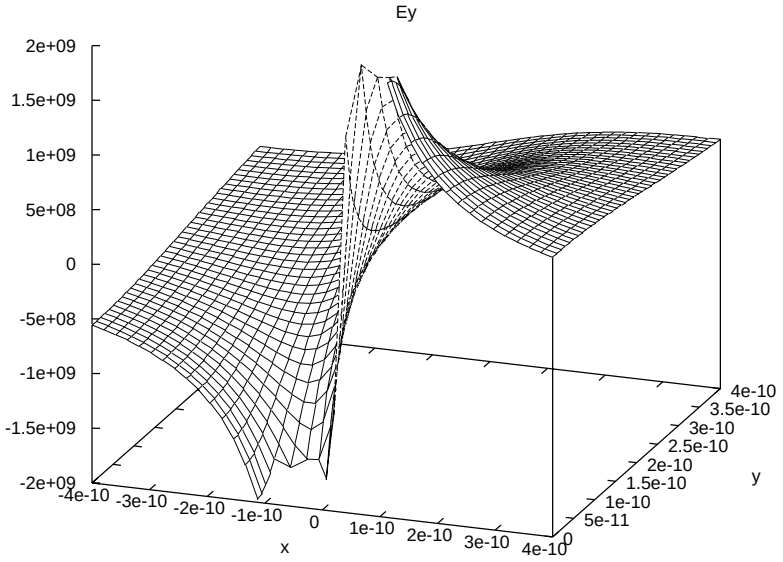

Figure 5.6: Spatial variation of electric field component E_y, with the $E_{extract}$ component removed (values in SI units)

Since it is not known what value of t we need to use to check the position coordinates, a routine is used to home in on the time at which the electron is at the height of the detector, by guessing either side until we are within a given margin of error. The 'guesses' are re-used for the next electron, to try to minimise the number of guesses needed, and speed up the simulations.

5.2.5 Analysis

The results are mainly given in the form of percentage detection profiles against position. The profiles do not always form an obvious plateau either side of the junction, so to find a contrast value we have take the intensities at arbitrary positions. We chose $\pm 1\mu m$ and $\pm 5\mu m$ as being in general representative of the contrast. The contrast was then calculated as below:

$$C(pn) = \frac{S(p) - S(n)}{S(n)}$$

This definition is the one used by Sealy *et al.* For the ionisation contrast, we expect the contrast thus defined to be positive.

5.3 Simulations

The above process can then be run on a complete distribution of electrons to get a percentage detection, which corresponds to a single data point. Simulations can be run on a whole range of values of $x_0 = x(t = 0)$, the excitation point, to scan across the p-n junction and produce a plot from which contrast across the junction can be calculated. Other parameters such as the extractor voltage can then be varied.

First of all, the model was tested for robustness to arbitrary choices made in the program. For example, the value of $y_0 = y(t = 0)$ cannot be chosen as

zero, due to the singularity in the potential here. We therefore checked that the model would give the same results over a sensible range of y_0, from 10^{-12}m to 10^{-9}m, and it was found to give almost identical results. Similarly the results were very similar for slightly different detection algorithms.

We then calculated how the detection profile varied with different values of V_{BI} and different values of ϕ. We homed in on the values that would be correct for a typically doped silicon p-n junction ($V_{BI} = 0.7V, \phi = 4.52eV$), and then calculated the profile for a large range of extractor biases. From this a plot of contrast against $V_{extract}$ was produced.

5.4 Results

As a sanity check, we have included a plot of electron trajectories generated in one of the simulations. The plotting was done using `MuPAD` by making a few additions to the program. See figure 5.7.

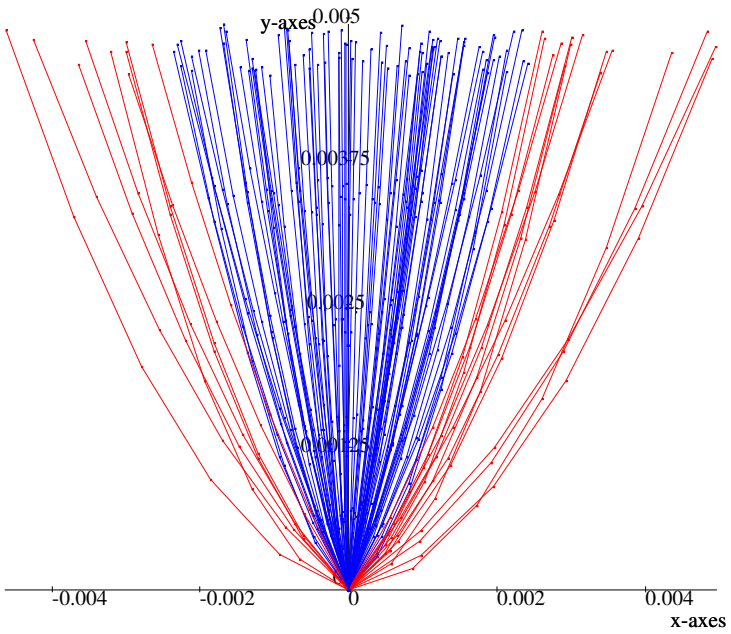

Figure 5.7: Example plot of electron trajectories from a simulation. About 100 trajectories are plotted here—for each data point about 350 were calculated. Axes are labelled in metres.

5.4.1 Effect of ϕ

Figure 5.8 shows the results obtained for the profile with different values of material work function. The value of V_{BI} used was 0.7 V, as used for the remainder of simulations.

Calculated values of contrast from these plots can be seen in figure 5.9.

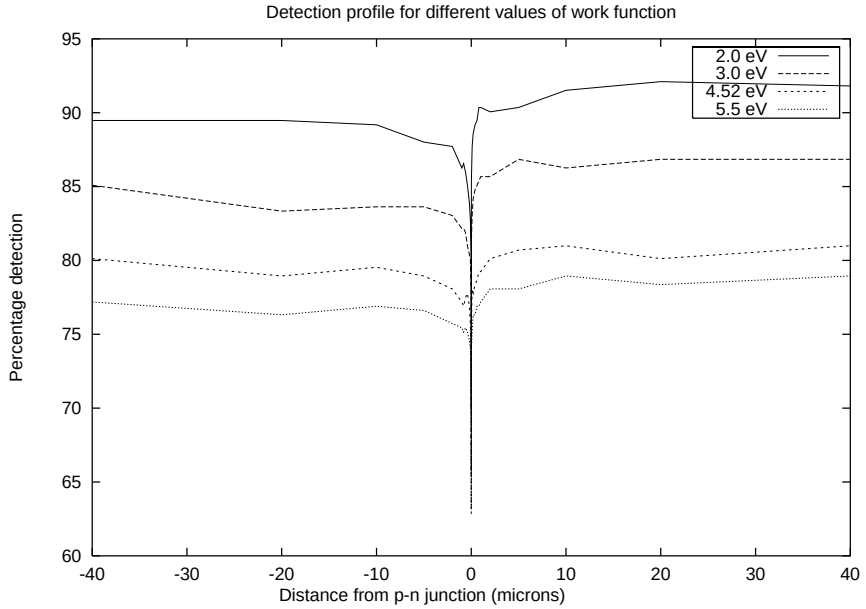

Figure 5.8: Theoretical percentage detection against position for various values of ϕ, for $V_{BI} = 0.7$ V

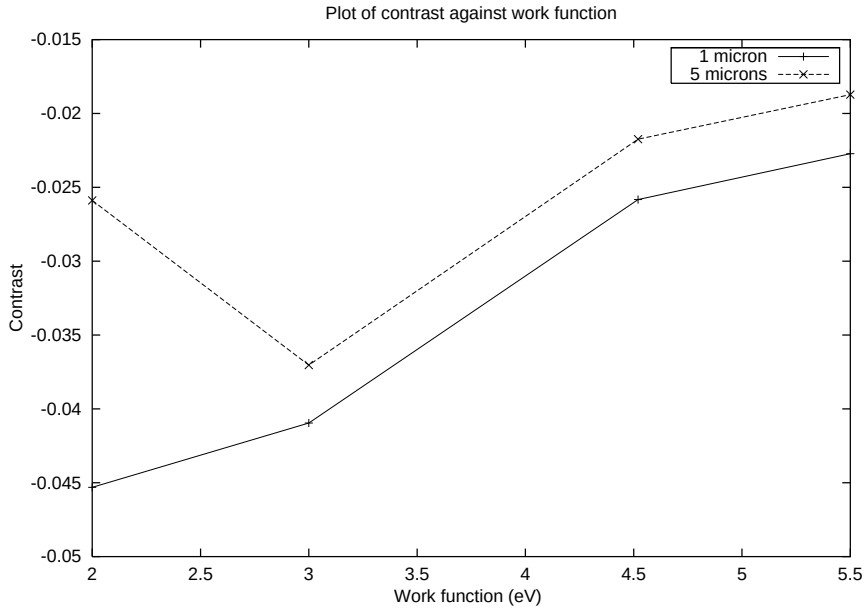

Figure 5.9: Theoretical contrast against ϕ, for $V_{BI} = 0.7$ V

5.4.2 Effect of V_{BI}

Figure 5.8 shows the results obtained for the profile with different values of built-in voltage (which corresponds to different doping levels). The value of ϕ used was 2.0 eV.

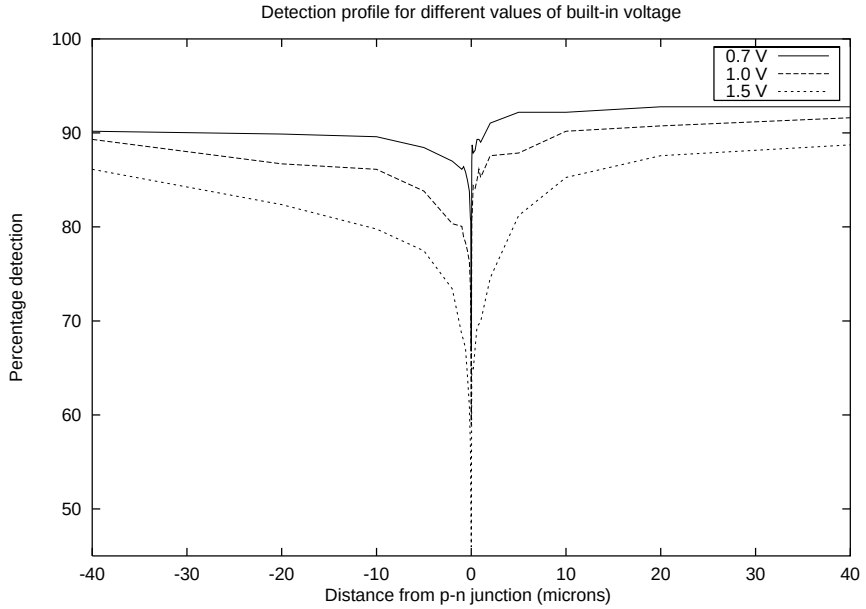

Figure 5.10: Theoretical percentage detection against position for various values of V_{BI}, using $\phi = 2.0$ eV

5.4.3 Effect of $V_{extract}$

More work was done on this variable than the other two. The plots of the percentage detection profile can be found below. It was found that for $V_{extract} > 140V$, the fraction detected saturated to 100%. Therefore only plots from below this value are shown. A plot of the contrast for different values of $V_{extract}$ is shown in figure 5.12.

5.5 Discussion

From the spatial variation of E_x (figure 5.5, page 21), it can be seen that for a negatively charged particle there will always be a positive force in the x–direction, i.e. a force to the right. This force peaks close to $x = 0$, $y = 0$. Therefore we expect the electrons to be deflected to the right, particularly when close to the p-n junction, and thus a decrease in the fraction detected around this region. This does not predict any contrast betwen the two sides.

However, electrons emitted from the p-side will be pushed to the right into regions where the field is *stronger*, and so will be accelerated faster to the right. Electrons emitted from the n-side will be also be pushed right, but on this side the field *decreases* with increasing x, and so the electrons are deflected less (see figure 5.13). Thus we expect more deflection, and thus less electrons reaching the detector, for the p-type than for the n-type side of the junction. This would give rise to a negative contrast (which is observed in most cases).

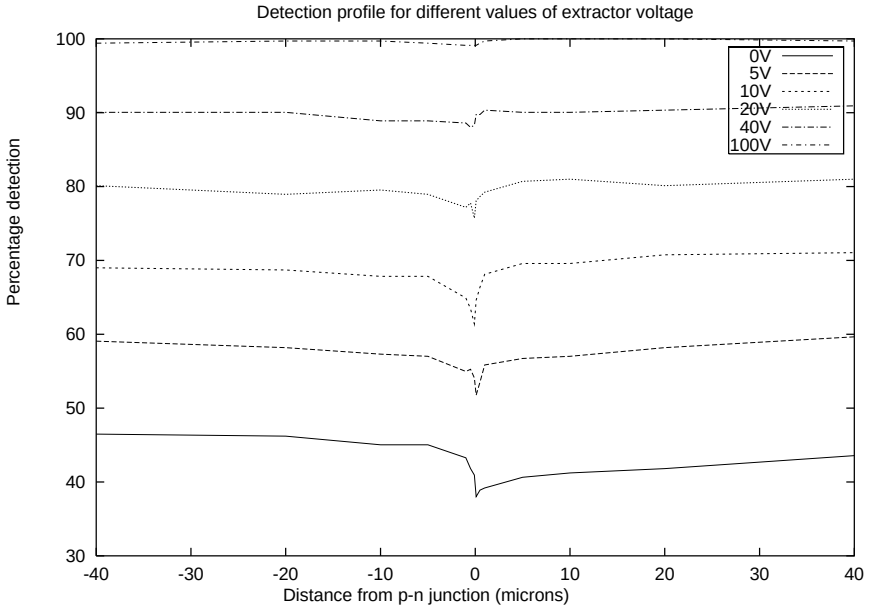

Figure 5.11: Theoretical percentage detection against position for various extractor biases, using $\phi = 4.52$ eV and $V_{BI} = 0.7$ V

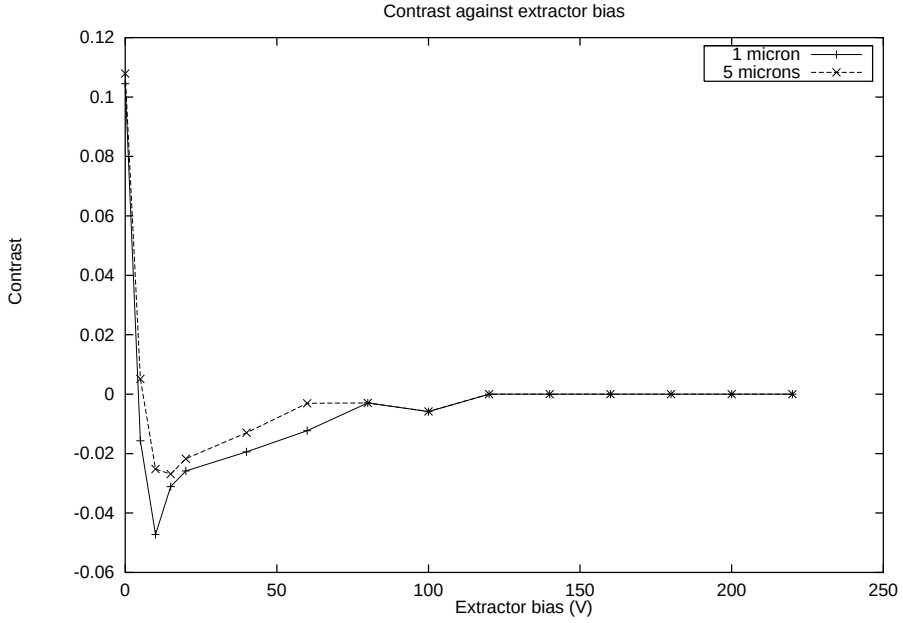

Figure 5.12: Theoretical contrast against extractor bias

In this explanation, we have ignored the E_y component, but for most extractor voltages the component of E_y due to the p-n junction is negligible compared to $E_{extract}$.

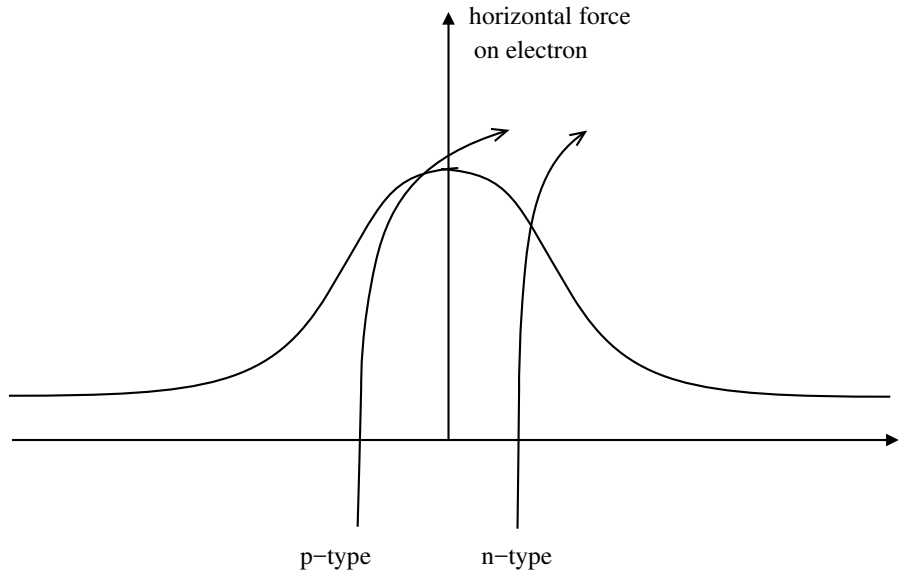

Figure 5.13: Diagram to illustrate the different effect of the horizontal component of force on electrons either side of the junction. Two electron trajectories are overlaid onto the plot—the electron on the left is pushed into a region of higher horizontal force, and thus deflected even more.

Note that we have assumed that deflection will, in general, cause electrons to be *less* likely to reach the detector. For some electrons this assumption is clearly false (i.e. those with trajctories that naturally would have moved to the left of the detector, and are moved towards it by the field). However, we can say from the probability distribution that these electrons are fewer in number than those that head approximately vertically, and also their initial trajectory will not take them as close to the large peak in E_x close to the origin, and so they will probably be less affected by the field, and so in attempting to understand this we should concentrate on those with angles close to zero.

The results, for the most part, accord well with these predictions. All of the plots show a decrease in the yield close to the interface between p- and n-type material. The prediction concerning the sign of the contrast is also generally true, as can be seen from figure 5.11 and others.

5.5.1 Effect of ϕ

Increasing the work function will produce a distribution with higher energies (see section 5.2.1). We might therefore expect that a greater number of electrons will be able to escape, and so the overall percentage detection will go down, which is exactly what is observed in figure 5.8. Note that this is the percentage detection of those electrons emitted—it does not take into account the number of electrons emitted, which varies strongly with work function. How this effects the contrast is not easy to predict, nor do the results show a clear enough pattern to be analysed (the values of contrast taken at $\pm 1\mu m$ and $\pm 5\mu m$ vary significantly).

5.5.2 Effect of V_{BI}

The results show that as the value of V_{BI} is increased, the dip in percentage detection at the p-n junction becomes much deeper and broader. This is consistent with the predictions above: the electric field E_x is proportional to V_{BI}, and so we expect greater deflection of electrons as V_{BI} is increased, and thus lower detection rates. If this mechanism is genuinely operating, then by using high dopant concentrations (and thus high built-in voltages), the dip in detection at the interface between p and n should become easily visible, even if the actual contrast is masked by other mechanisms, and this provides a good way to test this work experimentally.

5.5.3 Effect of $V_{extract}$

As already mentioned, the contrast for most values is negative, as expected. For example, for $V_{extract} = 20$ V, there is a negative contrast of about -2.5%. This contrast decreases (in magnitude) with increasing $V_{extract}$, as expected, due to the patch fields being made negligible compared to the extractor field.

However, for very low $V_{extract}$ the contrast, instead of become large in magnitude (more negative), actually reverses. This can be explained in terms of E_y, which is now mainly or entirely composed of the E_y due to the p-n junction (see figure 5.6, page 22 for a plot of this). This component now represents a large attractive force for positive x (p-side of the junction), and a large repulsive force for negative x (n-side). The electrons emitted from the p-type material are thus accelerated to the detector, and from the n-type they are attracted back to the surface. This results in the large positive contrast seen. This effect now adds to the contrast that would be seen for the mechanism described by Sealy. However, in the experimental results obtained, there is in fact a drop in contrast at $V_{extract} = 0$, and this was also observed by Elliot[1]. This either suggests that an over-calculation of the size of this mechanism, or that it is other mechanisms that drop off at $V_{extract} = 0$.

Chapter 6

Conclusions

We have demonstrated by use of a computer model that the external patch fields generated on an unbiased p-n junction have a significant effect on the SEM dopant contrast observed, in terms of the effect on the trajectories of emitted electrons, and thus the detection rate of these electrons. For typical operating conditions, the effect is a negative contrast of aproximate magnitude 2%. However, at low extractor voltages, this mechanism can cause a positive contrast (p-type brighter than n-type) of up to 10%. These results have been explained in terms of the form of the patch fields.

The experimental results obtained were not very useful in either confirming or falsifying this theory, since this mechanism is not the major one. However, from the model it is predicted that the detection rate should drop close to p-n interface, and that this effect will increase with higher dopant levels. This provides a good way to test this mechanism. To date, this artefact does not appear to have been reported in any experiments, which is a serious concern. The reason might lie in the model of the patch fields. The model used ignores the presence of the space-charge region over which the potential decreases. The space-charge region is usually small, but ignoring it means that the potential on the surface is modelled as a step-function, which is clearly unrealistic. Since the electric field is the gradient of the potential, in the model the field becomes infinite at the junction, when in reality it will never exceed the built-in field. This means that the model will overestimate the size of the deflection of trajectories. This concern needs to be addressed and the results checked using a more realistic form of the potential.

There are a number of other ways in which the model could be improved:

- The 3D nature of the electron trajectories needs to be added, since the problem is not rotationally symmetric about the vetical axis. This is not thought to be a large error.
- Given that the computer program already calculates values of the speed of the electrons, a more sophisticated detection routine could easily be added that checks the energy of the electrons and applies some energy filtering criteria to mimic those of the detector.

The results obtained were taylored for a specific situation and machine, but the principles should be applicable more widely.

Bibliography

[1] Elliot SL, *Dopant Profiling With The Scanning Electron Microscope*, Cambridge University Press

[2] Plows GS, (1969) *Stroboscopic Scanning Electron Microscopy and the observation of microcircuit surface voltages*, University of Cambridge

[3] Lifshin E, DeVries RC (1972), Anomalous contrast effects encountered in SEM studies of cubic boron nitride in *Proceedings 7th Conference on Electron Probe Analysis*, EPASA, San Francisco, 18A-18B

[4] Aven M, Devine JZ, Bolon RB and Ludwig GW (1972) Scannin electron microscopy and cathodoluminescence of ZnSexTel-x p-n juntions, *Jnl of Applied Phys*, **43**(10) 4136-4141

[5] Perovic DD, Castell MR, Howie A, Lavoie C Tiedje T and Cole JSW (1995) Field-emission SEM imaging of compositional and doping layer semiconductor superlattices, *Ultramicroscopy*, **58** 104-113

[6] Reimer L, *Scanning Electron Microscopy—Physics of Image Formation and Microanalysis*, Springer-Verlag.

[7] Sealy CP, Castell MR and Wilshaw PR (1999) *Mechanism for secondary electron dopant contrast in the SEM*, Deparment of Materials, University of Oxford.

[8] Dalven R, *Introduction to applied solid state physcis*, 2nd edition, Plenum Publishing Corporation.

Appendix A

Source Code

This was in 3 parts. The first is a settings file. The second is main program, and the third was a script that generated the settings file and then ran both the settings file and program through MuPAD. Included below is a sample setting file and main program. Note that the program went through several versions as new features were added.

```
Sample settings file
--------------------
numAngBins:=10:
numEv:=400:
extractorVoltage:=15:
numEnBins:=20:
DIGITS:=8:
V_BI:=0.7:
y0:=10^(-12):
HISTORY:=0:
wd:=4.5*10^(-3):
angRange:=PI:
workFn:=4.52:
datafilename:="intensity_vs_expt_exvolt_15":
exPt:=1*10^(-6):
tFin:=2*10^(-9):

Main program
------------
/* -*- mupad -*- */

print(Unquoted,"Running prog_main3.mu...");

q_e := -1.60*10^(-19):
m_e := 9.11*10^(-31):

extractorField := -extractorVoltage/wd:
V := (x,y) -> V_BI/PI * arctan(x/y) - extractorField*y:
E_x := -D([1],V):
E_y := -D([2],V):
E_z := 0:
pAngle := a -> cos(a):
pEnergy := en -> en/(en+workFn)^4:
/* renormalised probability function (can renormalise the two components separately
as they are functions of one variable only) */
n1:= int(pEnergy(en),en=0..infinity,Continuous):
n2:= int(pAngle(alpha),alpha = -PI/2..PI/2):
```

```
prob := (alpha,en) ->  pEnergy(en)*pAngle(alpha)/(n1*n2):

// We want to scale the energy range so that we get an self similar
// distribution of energies whatever the work function.
// Scale it so that we have at most 1 electron in the box
// that is at energy = enRange.
//
// We require zero electrons in the box that would be at en=enRange,
// alpha=0.  This requires prob(0,enRange) * area of the box * numEvents < 0.5:
// prob(0,enRange) * numEv * enRange/numEnBins * angRange/numAngBins < 1/2
// since < 0.5 would be rounded down to 0
// Using a symbolic integration on n1 above, it can be shown that the
// equation we need to solve is:

// 6*(enRange*workFn)^2 * numEv * angRange
//   - numEnBins*numAngBins*(enRange+workFn)^4 = 0

eqn:= (6*(enRange*workFn)^2*numEv*angRange
      - numEnBins*numAngBins*(enRange+workFn)^4 = 0):
solns:= solve(eqn,enRange):

// Then get the largest value
emax:=max(eval(float(solns))[i] $ i=1..nops(eval(float(solns)))):

// NB don't assign to  enRange on the LHS, because as far as MuPAD is
// concerned it is also on the right hand side, which confuses it

// There is a possibility of failure if the left hand side of eqn
// never reaches  1/2.  This// is because numEv is too small for the
// number of bins.  Issue error message and die. (the complicated
// boolean is because emax will be neither positive or negative, but
// unknown)

if (not(is(emax, Type::Positive) = TRUE)) then
  error("An error occurred.  This is probably because the value of
         numEv is small compared with the product numEnBins*numAngBins.");
end_if:

enRange:=emax:

da:= float(angRange/numAngBins):
den:= float(enRange/numEnBins):
EvArray:= matrix(numEnBins,numAngBins):
rand5:= float(random(0..99999)/100000):

//  Cut the probability distribution into bins, and put electrons
//  in each bin.  Perhaps this method should be randomised with
//  a poisson distribution, so that there is some chance of getting an
//  electron with a higher energy (at the moment there is none)
//

for i from 1 to numEnBins do:
  for j from 1 to numAngBins do:
    // we need to do a double integration here, but that is tricky
    // and takes a long time!
    // Get a good enough numerical approx by averaging the height at the four
    // corners and multiplying by the base area
    // Note that we need to multiply by numEv so that our total
    // number of electrons approx= numEv
```

```
    EvArray[i,j] := float(prob(-PI/2+(j-1)*da,(i-1)*den)) +
      float(prob(-PI/2+j*da,(i-1)*den)) +
      float(prob(-PI/2+(j-1)*da,i*den)) +
      float(prob(-PI/2+j*da,i*den)):
    EvArray[i,j] := round(eval(EvArray[i,j]/4*da*den*numEv)):
  end_for:
end_for:

// Get table of angles and energies of electrons
// Each electron is given an energy and angle randomly slected from
// within the bin it is in.

angTable:=table():
enTable:=table():
l:=1:

for i from 1 to numEnBins do;
  for j from 1 to numAngBins do;
    for k from 1 to EvArray[i,j] do:
      angTable[l]:=-PI/2+(j-1+rand5())*da:
      enTable[l]:=(i-1+rand5())*den:
      l:=l+1:
    end:
  end:
end:

numElectrons:=l-1 : print (Unquoted,"numElectrons:"):
print(numElectrons):

// these convert energies _in_electron_volts_ to
// velocities vx,vy.  Theta is the angle from the y axis
vx:= (theta,en) -> sqrt(2*abs(q_e)*en/m_e)*sin(theta):
vy:= (theta,en) -> sqrt(2*abs(q_e)*en/m_e)*cos(theta):

// This method won't work (just a bit too hard for MuPAD!):
//eqn:=ode({
//  x''(t) = q_e/m_e * E_x(x(t),y(t)),
//  x'(0)  = vx(alpha,en),
//  x(0)   = exPt,
//  y''(t) = q_e/m_e * E_y(x(t),y(t)),
//  y'(0)  = vy(alpha,en),
//  y(0)   = 10^(-12)},
//  {x(t),y(t)} );
// solve(eqn);

// so rewrite as a first order:
//   if we define: Y=[x,x',y,y']
//   can write:    Y'=f(Z,t)  - now it is first order
//   specifically:
//   Y'=[Y[2],
//       q_e/m_e*E_x(Y[1},Y[3]),
//       Y[4],
//       q_e/m_e*E_y(Y[1],Y[3])]

f1 := (t,Y) -> [ Y[2],
                 q_e/m_e* E_x(Y[1],Y[3]),
                 Y[4],
                 q_e/m_e* E_y(Y[1],Y[3])]:
```

```
print(Unquoted,"Excitation point, x:");
print(exPt);

// Detection area:
detHeight:= wd:  // about right
detWidth := 2.5*10^(-3):

numDet := 0:
tGuess2 := 0:
usetGuess2 := FALSE:
t0 := 0:

for i from 1 to numElectrons do;
  print(Electron, i);
  en:=enTable[i]:
  alpha:=angTable[i]:
  Y0 := [exPt,vx(alpha,en),y0,vy(alpha,en)];
  Y := numeric::odesolve2(f1,t0,Y0);

// Collection routine:

// Try to guess at what time we are going to detect the electron
// Start with some defaults
  tGuess := tFin:
  tMax := 0:
  tMin := 0:
  tGiveUp := .01:
  // give up after a 1/100 second - this is only going to be used if there
  // is no extractor field, in which case the electron can go down (-ve y)
  numGuesses :=0:
  while TRUE do:
    numGuesses := numGuesses + 1:
    Y1:= Y(tGuess):
    if Y1[3] > detHeight then
      if Y1[3]/detHeight > 1.1 then
tMax := tGuess;
tGuess:=float((tMin + tMax)/2):
      else
if abs(Y1[1]) < detWidth then
  print (Unquoted,"detected!");
  numDet:=numDet+1:
end_if:

tFin := tGuess:
tGuess2 := tMin:
usetGuess2 := TRUE:

break:
      end_if:
    else
      // give up routine:
      if tGuess > tGiveUp then
// don't bother saving any values
break:
      end_if:

      // increase the miniumum value to what we are
      // currently on
      if tGuess > tMin then
```

```
tMin:= tGuess:
      end_if:

      // if we have no idea what tMax is, then
      // just double current tGuess
      if (tMax = 0) then
tGuess:= tMin*2:
      else
// otherwise use the saved tMax from last time through:
//   either from the previous electron...
if (tGuess2 > 0 and usetGuess2) then
  tGuess := tGuess2:
  usetGuess2 := FALSE:
else
        //   ...or from a previous guess that was too large.
  tGuess:= (tMin + tMax)/2:
end_if:
      end_if:
    end_if:
  end_while:
end_for:

// save the data
outdata:=fopen(Text,datafilename,Append):
fprint(outdata,float(exPt),float(numDet/numElectrons),numElectrons):
print(numDet);
print(numElectrons);
fclose(outdata):

quit:
```